Supporting Information

Anisotropic Electronic Coupling in Three-Dimensional Assembly of $CsPbBr_3$ Quantum Dots

Kazushi Enomoto*[1], Retno Miranti[1], Jianjun Liu[1], Rinkei Okano[1], Daishi Inoue[1], DaeGwi Kim*[2], Yong-Jin Pu*[1]

[1]RIKEN Center for Emergent Matter Science (CEMS), Wako, Saitama 351-0198, Japan.
[2]Department of Physics and Electronics, Osaka Metropolitan University, Osaka 558-8585, Japan
E-mail: kazushi.enomoto@riken.jp, kimtegi@omu.ac.jp, yongjin.pu@riken.jp

Experimental Section

Materials and Methods

Materials

Acetone (>99.0 %), ethyl acetate (>99.0 %), and toluene (>99.5 %) were purchased from FUJIFILM Wako Pure Chemical Co. (Osaka, Japan). Toluene (optical spectroscopy grade, >99.7 %) was purchased from Kanto Chemical Co. Ltd. (Tokyo, Japan). Cesium carbonate (99.9 %, Cs_2CO_3) was purchased from Sigma-Aldrich Japan K.K. (Tokyo, Japan). 1,3-Diaminopropane (>98.0 %, DAP), 1,2-ethane dithiol (>99.0 %, C2DT), 1,3-propane dithiol (>97.0 %, C3DT), 1,4-butane dithiol (>97.0 %, C4DT), 1,5-pentane dithiol (>95.0 %, C5DT), 1,6-hexane dithiol (>97.0 %, C6DT), 1,10-decan dithiol (>98.0 %, C10DT), 1,4-benzen dithiol (>98.0 %, BDT), and 4,4'-biphenyldithiol (>98.0 %, BPDT) were purchased from Tokyo Chemical Industry Co., Ltd., Tokyo, Japan. All the chemicals mentioned above were used as received. Lead(II) bromide (≥98 %, $PbBr_2$), oleic acid (technical grade 90 %, OA), oleylamine (technical grade 70 %, OAm), 1-octadecene (technical grade 90 %, ODE), and anhydrous diethylene glycol dimethyl ester (99.5 %) were purchased from Sigma-Aldrich Japan K.K. (Tokyo, Japan).

The ODE was used after N_2 bubbling for 15 min. The OA was purified by recrystallisation. 50 ml of OA was placed in a freezer for 15 min, and the remaining liquid was removed. The remaining solid was melted at room temperature. The freezing and melting cycles were repeated thrice. The purified OA was stored in a refrigerator.

Synthesis of $CsPbBr_3$ QD

$CsPbBr_3$ QDs were synthesized following the literature with modifications[1]. In a 25 mL three-neck flask, 0.83 mL of OA (2.63 mmol) and ODE (10 mL) were combined and heated at 120 °C

under vacuum for 1 h. Subsequently, 271 mg of Cs_2CO_3 (0.83 mmol) was introduced under N_2 pressure, and the mixture was dried under vacuum for 1 h to produce a solution of cesium oleate. The setup was then switched to an N_2 atmosphere and heated at 160 °C.

A mixture of 10 mL of OA (32.0 mmol), 10 mL of OAm (31.0 mmol), and 100 mL of ODE in a predried 200 mL three-neck flask was heated at 120 °C under vacuum for 1 h. First, 1380 mg of $PbBr_2$ (3.6 mmol) was added under N_2 pressure, and the mixture was dried under vacuum for 1 h. After the system was switched to N_2 atmosphere conditions, the mixture was heated at 170 °C. Subsequently, 8.0 mL of caesium oleate solution was swiftly injected. After 5 s, the reaction mixture was placed in an ice bath.

For purification, 1.4 mL the crude dispersion was centrifuged at 12,000 rpm for 15 min, and the supernatant was discarded. The precipitate was redispersed into 500 μL of toluene and centrifuged at 12,000 rpm for 15 min. The obtained supernatant was mixed with 750 μL of ethyl acetate and centrifuged at 12,000 rpm for 15 min. The precipitate was redispersed into 300 μL of toluene and centrifuged at 12,000 rpm for 5 min. The collected supernatant was treated with ammonium thiocyanate (ATC) [2]. The ATC-treated $CsPbBr_3$ QDs solution was then stored in a refrigerator.

Layer-by-Layer assembly of $CsPbBr_3$ QD

The packing density and electronic coupling in $CsPbBr_3$ QD films can be regulated by varying multiple parameters. A common preparation method involves spin-coating a PEI water solution onto quartz treated with UV-ozone at a rate of 2,000 rpm for 30 s, followed by vacuum drying. The concentration of PEI was altered to control the thickness of the film. **Fig. S12** illustrates the impact of PEI concentration on the thickness and roughness of the PEI underlayers generated. X-ray refractometry (XRR) indicated that the thickness of the PEI underlayer increased linearly with an increase in PEI concentration, while surface roughness remained unchanged. For the LbL assembly of QDs, we adjusted the thickness of the underlayer to approximately 1 nm[3, 4]. Consequently, we chose a PEI concentration of 1.0 mg/ml to obtain a 1 nm thick underlayer.

The LbL assembly of $CsPbBr_3$ QDs was performed using a dip coater (KN4010 KSVNIMA Dip Coater Small, Multi-Vessel) in an N_2-flowing glovebox (humidity < 5 rh%). The monolayer of $CsPbBr_3$ QDs was fabricated by immersing a quartz substrate coated with PEI into a solution of $CsPbBr_3$ QDs for 5 min, followed by a vertical withdrawal at a controlled rate (0.01–9.9 mm/s) and a 5-min standing period for drying. To prepare the $CsPbBr_3$ QD multilayer, the substrate was alternately immersed in a linker solution and a $CsPbBr_3$ QD solution. Before the immersion in different solutions, the substrate was cleaned with hexane for 1 min and dried for 5 min to remove excess QDs or linkers.

Measurements

The UV-Vis spectra of $CsPbBr_3$ QD solution and film were recorded on a UV-3600 Plus (Shimadzu Co., Tokyo, Japan) using toluene as the solvent. The wavelength range was set at 300–800 nm, and the measurements were conducted at room temperature. All absorption spectra were collected with 0.2 nm step, which the minimum resolution is less than 1 meV in the range around the first excitonic peak. Fluorolog-3-TCSPC spectrofluorometer (HORIBA Ltd., Kyoto, Japan) was utilized to record PL and transient PL spectra. A pulsed laser source was used for the TrPL spectroscopy at 370 nm. The measurement of PLQYs of the samples was obtained using a C9920 instrument (HAMAMATSU PHOTONICS Co., Shizuoka, Japan), and the excitation wavelength was set to 450 nm. Furthermore, PL was measured using an integrating sphere system. TEM characterized the synthesized $CsPbBr_3$ QDs under an irradiation voltage of 200 kV (JEM-2100F/SP, JEOL Co., Tokyo, Japan) or 80 kV (JEM-1230, JEOL Co., Tokyo, Japan). The QD solution was deposited onto a Cu grid supported by a carbon-reinforced polyvinyl formal membrane (Okenshoji Co., Tokyo, Japan; PVF-C10 STEM Cu100P grid). Cross-sectional SEM was performed using a Quattro microscope (Thermo Fisher Scientific Inc., MA, USA). Cross-sectional specimens were prepared by utilizing the FIB method. Lastly, protective layers of osmium and carbon coatings were applied on the surface of the LbL film. In addition, EDX was performed using an EDXL300 spectrometer (RIGAKU Co., Tokyo, Japan), and the XRD measurements were conducted with a SmartLab (RIGAKU Co., Tokyo, Japan) using Cu Kα radiation.

Data analysis of XRD profile

To make clear the diffraction peaks in the in-plane direction (**Fig. S5**), detailed characterization was performed. The XRD profile was fitted with the following equation, $F(q)$ combined with the Gaussian and polynomial functions.

$$F(q) = \frac{1}{\sqrt{2\sigma^2}} \exp\left[-\frac{(q-\mu)^2}{2\sigma^2}\right] + \frac{a}{q^4} + \frac{b}{q^3} + \frac{c}{q^2} + \frac{d}{q} + e$$

Here, σ is the standard deviation, μ is the mean, and values of a, b, c, d, e is constant. All parameters were fitted by using least square method. Fitting curves are compared with experimental raw data, first derivative, and second derivative, shown in **Fig. S6**. The center-to-center interparticle distance was estimated from $2\pi/\mu$.

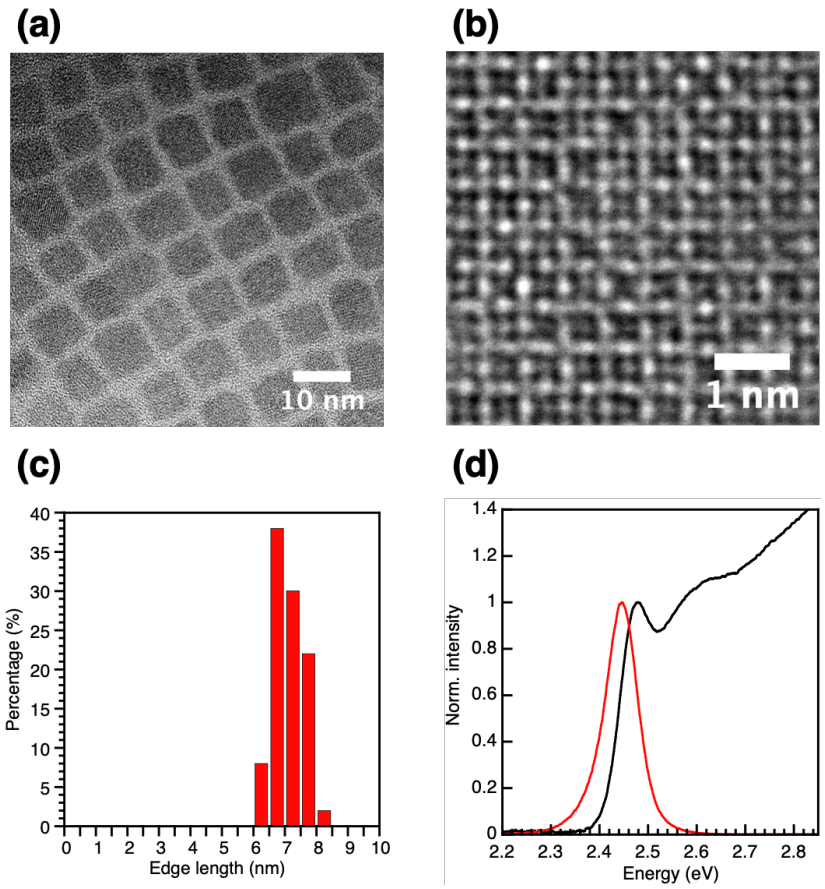

Fig. S1. Characterisation of synthesised perovskite quantum dots (PeQDs). **a)** Transmission electron microscopy (TEM) images, **b)** high-resolution TEM (HR-TEM) images, **c)** size histogram, and **d)** absorption and photoluminescence (PL) spectra of PeQDs.

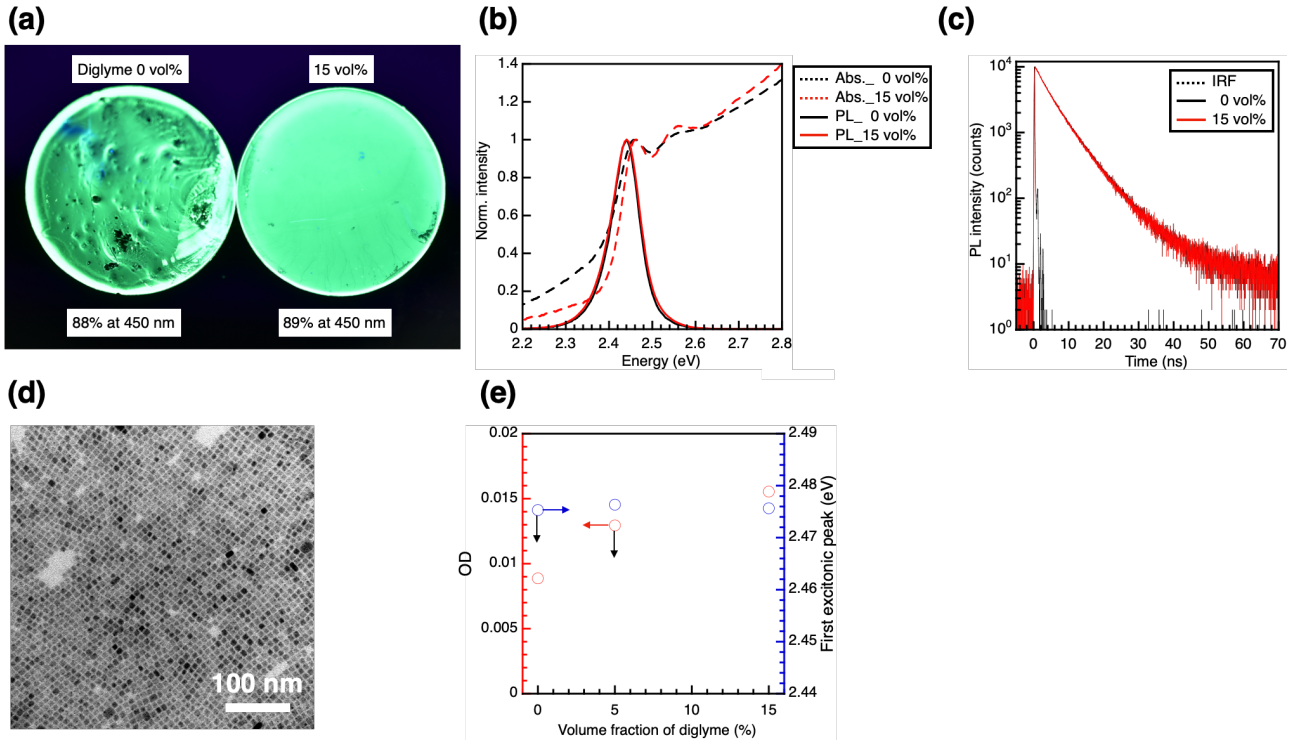

Fig S2. **a)** Photo of perovskite quantum dot (PeQD) films drop cast from toluene (left) and toluene/diglyme (85:15 v/v, right) solution. **b)** Absorption and photoluminescence (PL) spectra, and **c)** transient PL (TrPL) decays of PeQD solutions. **d)** Transmission electron microscopy (TEM) image of PeQD monolayer cast from toluene/diglyme solution. **e)** Effect of diglyme addition on optical density (OD) and first excitonic peak energy of PeQD monolayer.

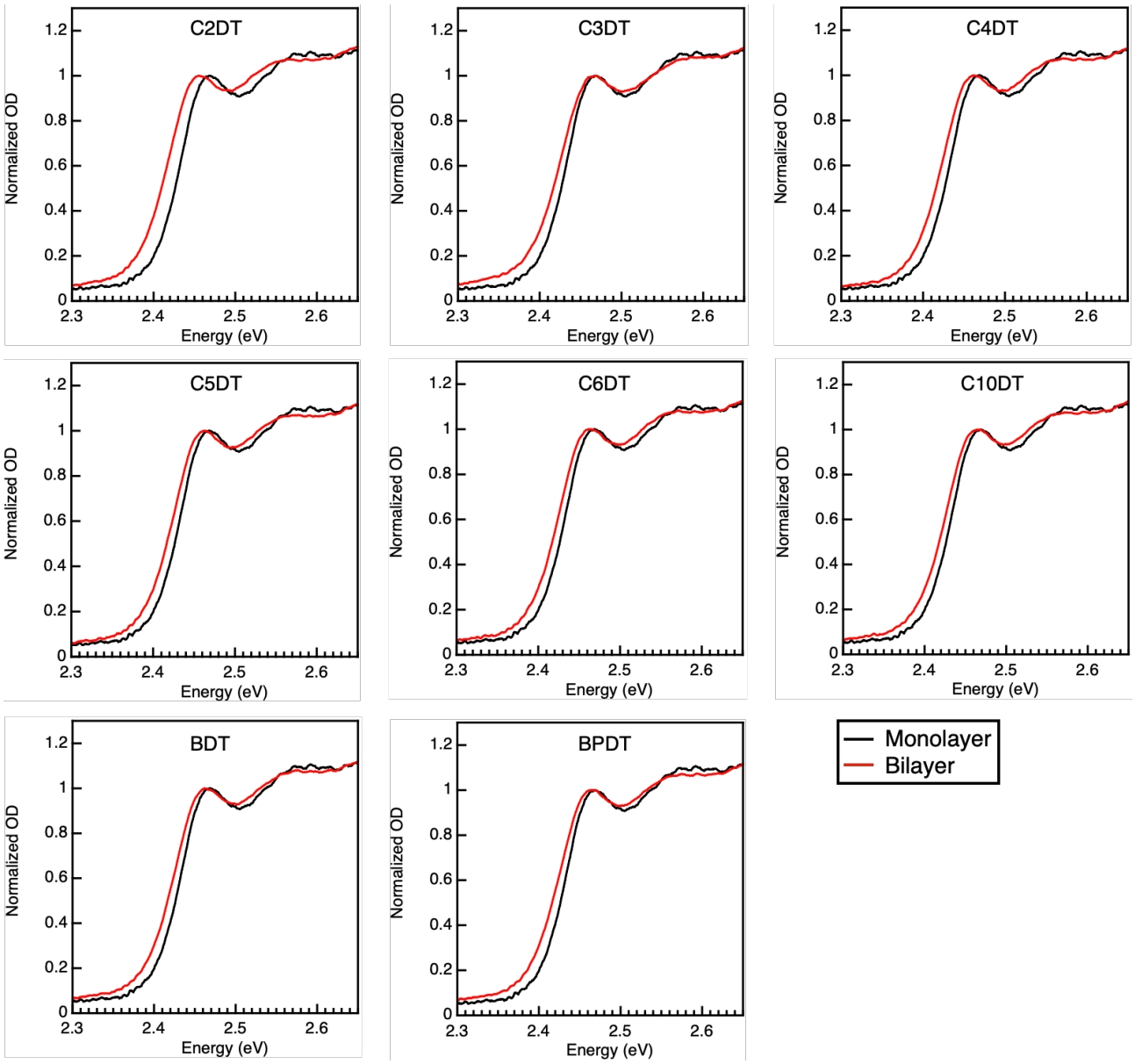

Fig. S3. Absorption spectra of the monolayer and bilayers formed using different types of alkane and aromatic dithiol linkers.

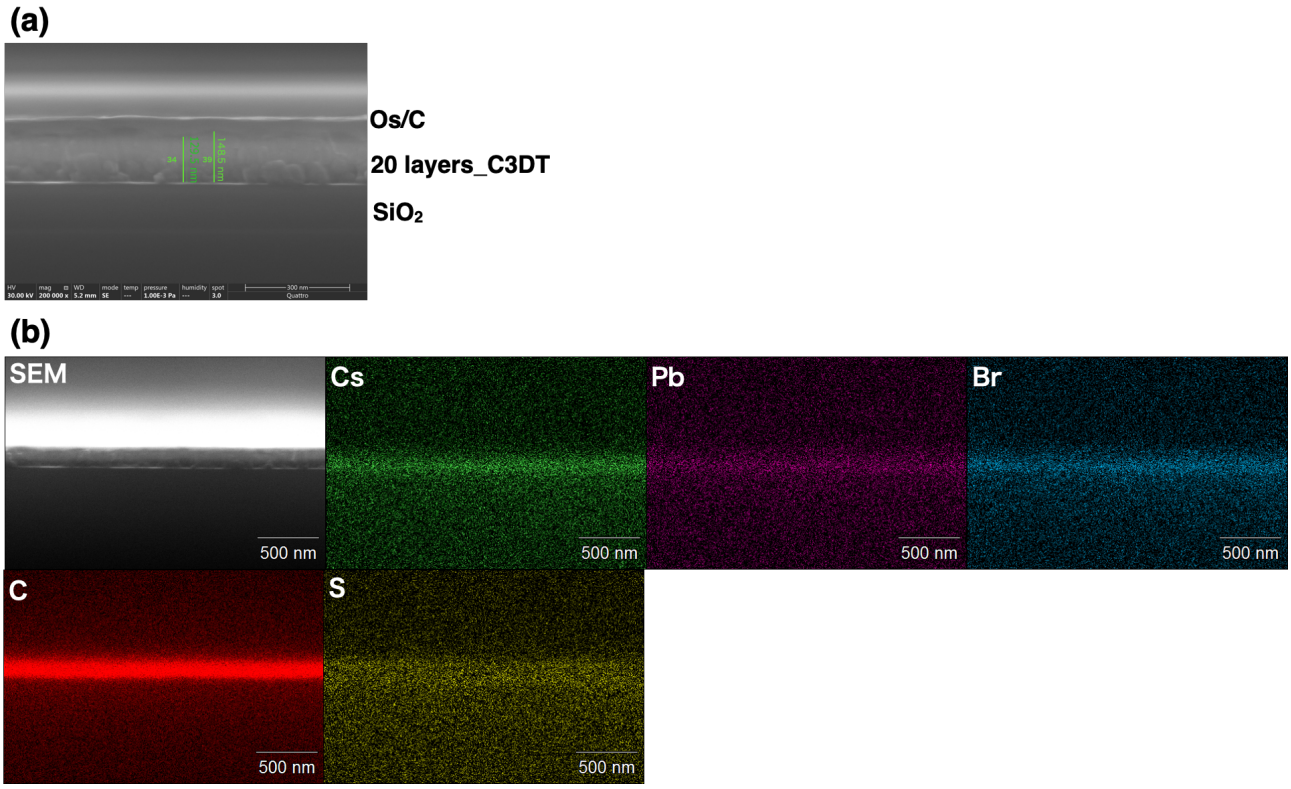

Fig. S4. Cross-sectional **a)** scanning electron microscopy (SEM) image, and **b)** SEM energy-dispersive X-ray spectroscopy (SEM-EDS) mapping of twenty layers prepared with C3DT.

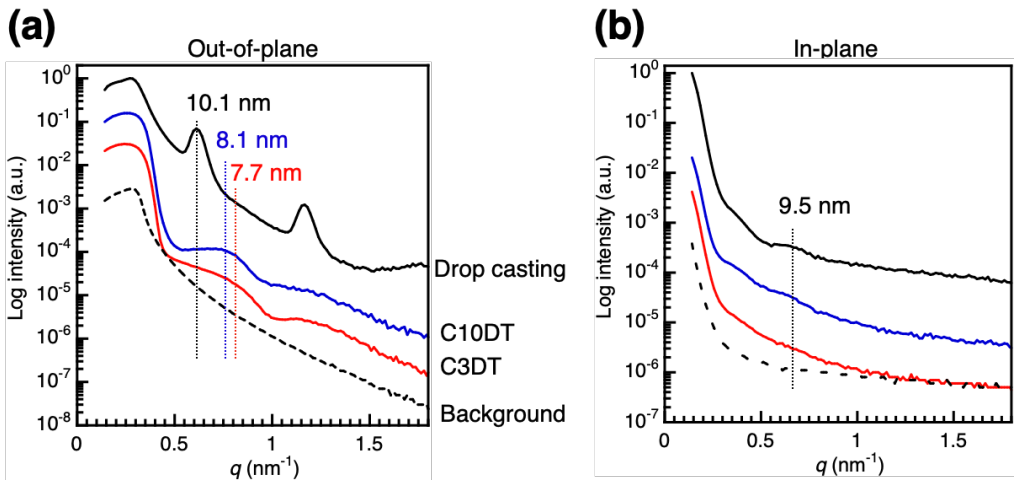

Fig. S5. X-ray diffraction (XRD) patterns of drop cast film, thirty-layer films prepared with C3DT and C10DT, and background in **a)** the out-of-plane and **b)** the in-plane direction.

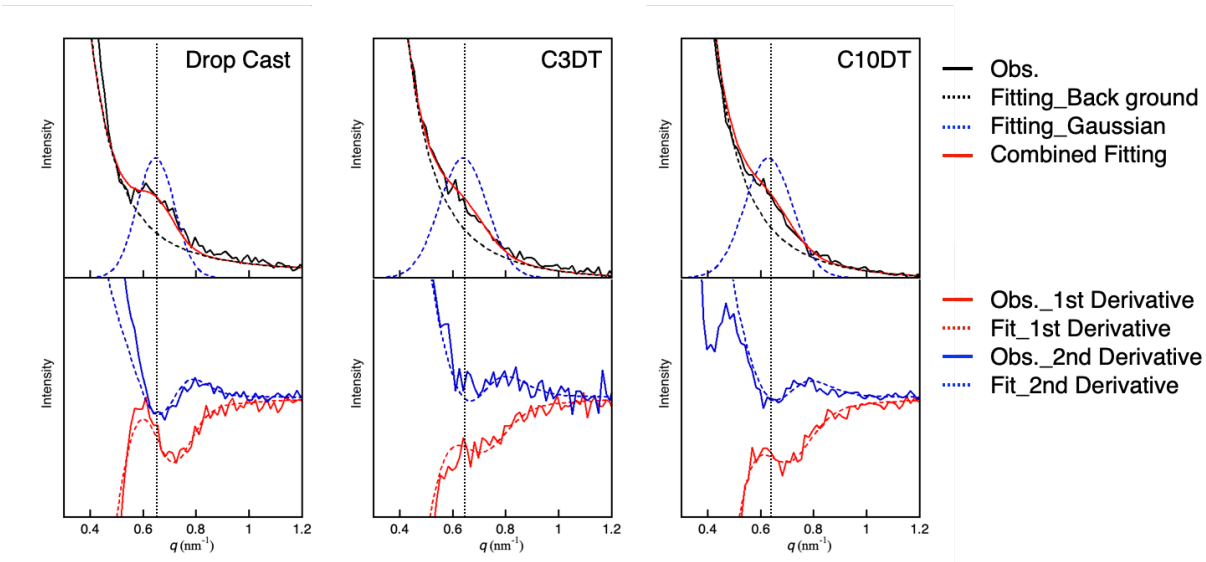

Figure S6. Diffraction peak analysis of in-plane XRD profiles. Upper figure; observed profile (black), fitting curve (red) combined with Gaussian function (blue dashed) and polynominal function for back ground (black dashed). Bottom figure; the first derivative (red) and the second derivative (blue) of observed (solid) and fitting (dashed) profiles.

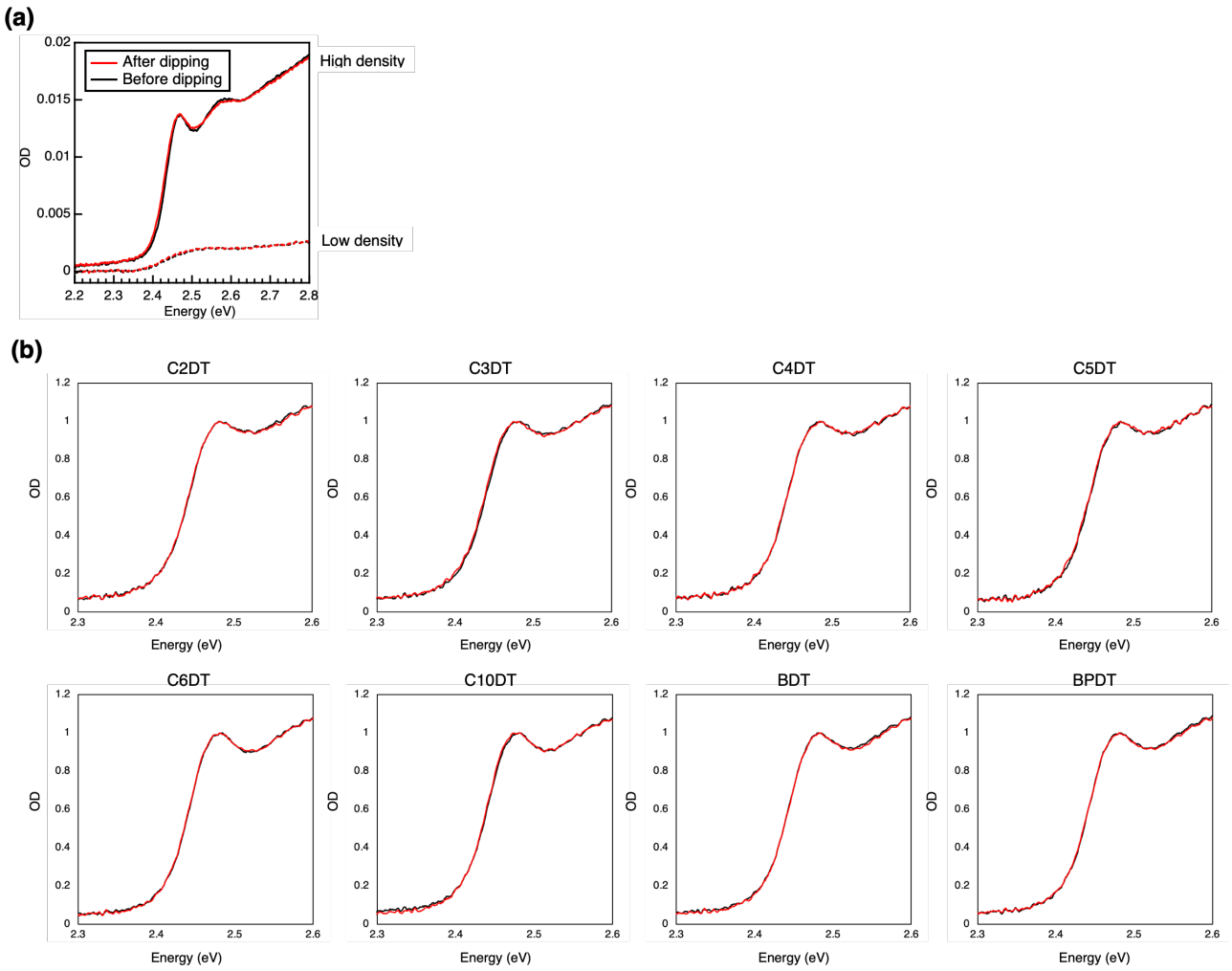

Fig. S7. (a) Comparison of absorption spectra of perovskite quantum dot (PeQD) monolayers with different particle densities before (black line) and after (red line) soaking into C3DT linker solution. **(b)** Comparison of absorption spectra of PeQD monolayers with high particle density before (black line) and after (red line) soaking into different types of dithiol linker solutions.

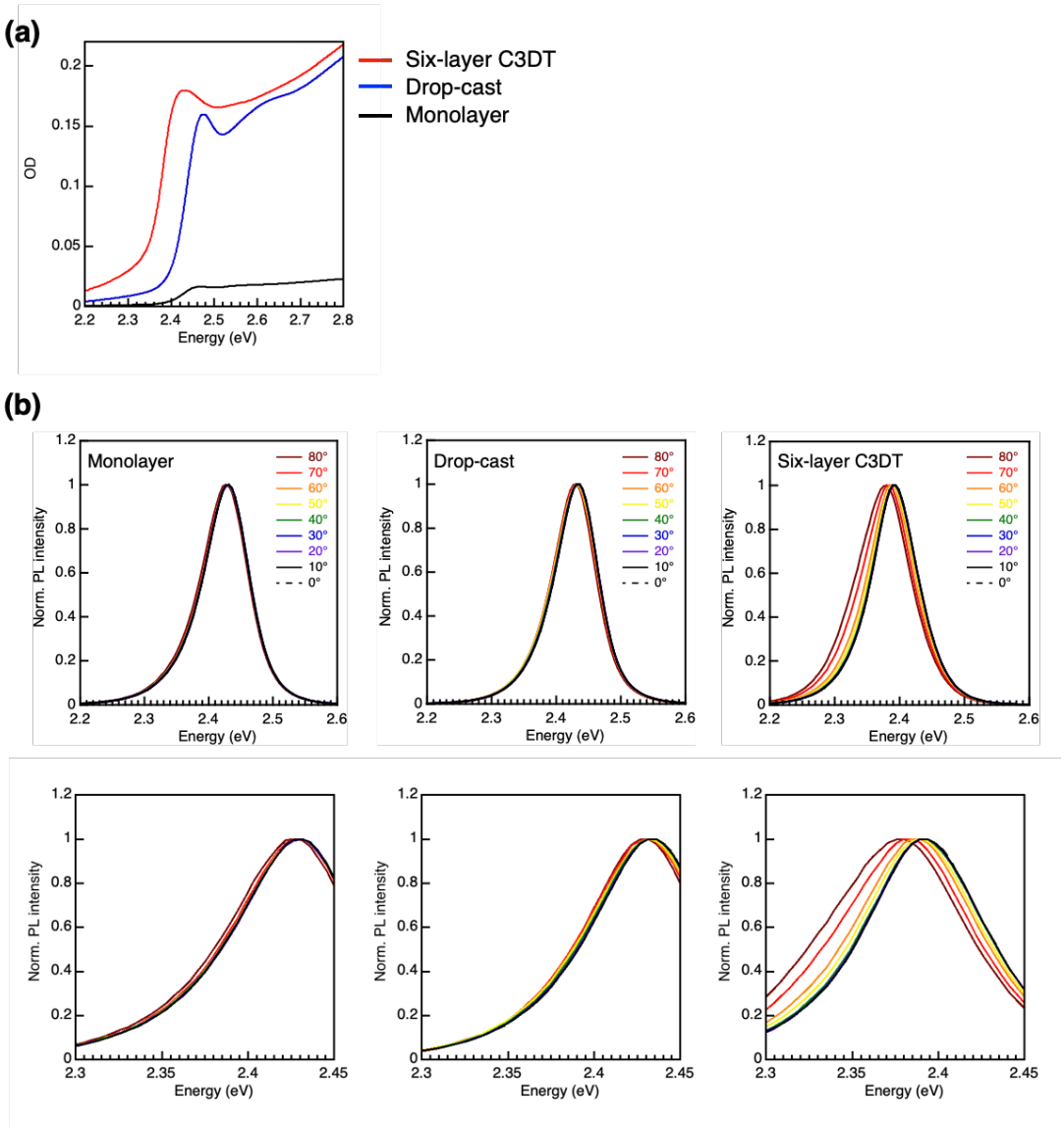

Fig. S8 a) Absorption spectra of monolayer, six-layer bridged with C3DT, and drop cast film for angle-dependent PL measurement. **b)** Angle-dependent photoluminescence (PL) spectra of monolayer, drop cast film, and six-layer bridged with C3DT. Upper line shows whole range and bottom line shows enlarged range.

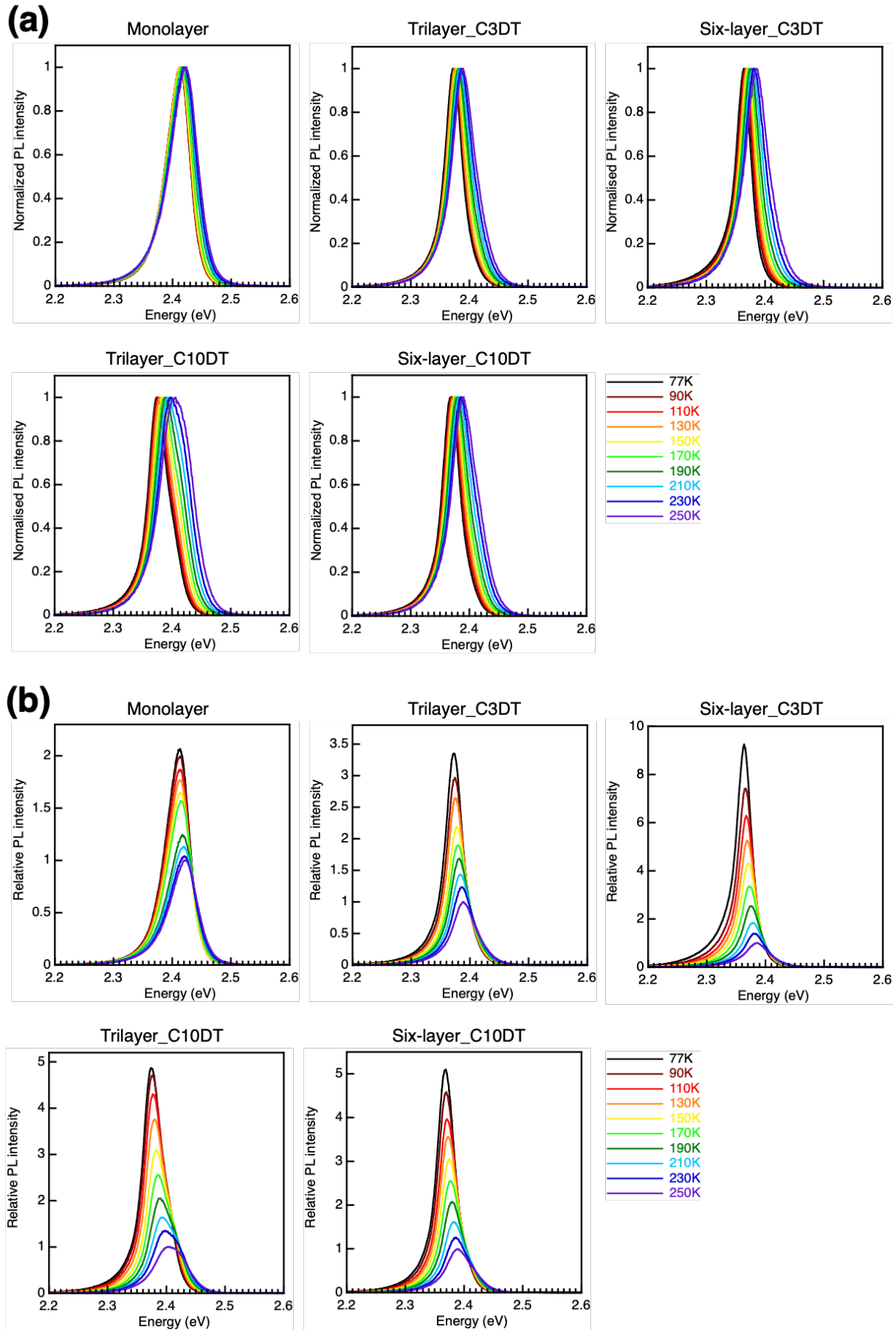

Fig. S9. Temperature dependence of **a)** normalized photoluminescence (PL) and **b)** relative PL spectra.

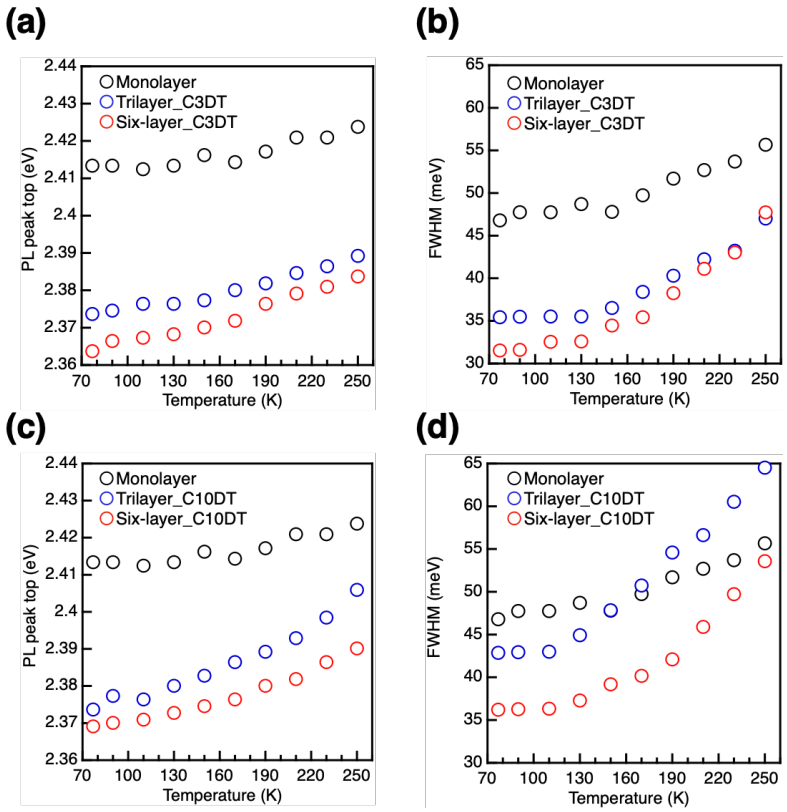

Fig. S10. Temperature dependence of **a)**, **c)** photoluminescence (PL) peak top energy and **b)**, **d)** full width at half maximum (FWHM) of perovskite quantum dot (PeQD) monolayer, trilayer, and six-layer prepared with **a)**, **b)** C3DT, or **c)**, **d)** C10DT.

Table S1. Parameters obtained by curve fitting using Eqs. 2. and 3 with variable and fixed E_{LO} values

		Monolayer	C3DT		C10DT		
			Trilayer	Six-layer	Trilayer	Six-layer	
	E_0	2.31	2.29	2.29	2.28	2.28	(eV)
	A_{TE}	0.1	0.0	0.1	0.1	0.0	(meV/K)
	A_{EP}	101	86	75	84	90	(meV)
	$\hbar\omega$	69	66	60	55	58	(meV)
	r^2	0.95	0.99	0.98	0.99	1.00	
E_{LO}= Variable	Γ_0	49	59	69	43	67	(meV)
	γ_{LO}	75	173	375	145	278	(meV)
	E_{LO}	47	35	32	42	36	(meV)
	r^2	0.97	0.99	1.00	0.99	0.99	
E_{LO}= 30 meV	γ_{LO}	26	31	60	67	41	(meV)
	Γ_0	46	34	29	41	35	(meV)
	r^2	0.96	0.92	0.95	0.98	0.95	
E_{LO}= 20 meV	γ_{LO}	14	15	33	34	21	(meV)
	Γ_0	46	34	27	40	34	(meV)
	r^2	0.94	0.88	0.93	0.96	0.92	
E_{LO}= 10 meV	γ_{LO}	6	6	14	14	9	(meV)
	Γ_0	45	33	24	37	33	(meV)
	r^2	0.92	0.85	0.92	0.94	0.89	

Table S2. Reported parameters of perovskite crystals with different sizes and shapes.

Sample	Size	E_0	A_{TE}	A_{EP}	$\hbar\omega$	Γ_0	γ_{LO}	E_{LO}	γ_{ac}	*ref*
	(nm)	(eV)	(meV/K)	(meV)	(meV)	(meV)	(meV)	(meV)	(μeV/K)	
Monolayer	6.8	2.31	0.1	101	69	49	75	47		This study
C3DT_3rd		2.29	0.0	86	66	59	173	35		
C3DT_6th		2.29	0.1	75	60	69	375	32		
C10DT_3rd		2.28	0.1	84	55	43	145	42		
C10DT_6th		2.28	0.0	90	58	67	278	36		
QD on sapphire substrate	3.9					86±2	89±27	23±6	22±50	5
	4.7					69±3	32±18	22±11	20±70	
	5.3					52±1.5	52±13	21±8	20±60	
	6.3					40±2.5	32±13	20±9	70±75	
Monolayer on TEM grid	~5	23				76	86		20	6
	~5	23				57	67		20	
	~7					0.4	42±50	16	8±3	7
Drop cast on SiO_2	~9.1					25.4±0.38	160.4±9.27	36.1±1.18		8
	11.4	2.8	0.32	400	80	32	130	30		9
Drop cast on SiO_2-coated Si	14		0.62	68			ca. 73	22		10
	15					20	45	19	5	11
Drop cast on SiO_2	15		0.14	35.1			35.14	14.23		
Nanocrystals	15	2.43	0.14	35.1	55.6		35.1	14.2		12
Nanoplatelets	3.5	2.51	0.21	-190	151.9		39.6	15.6		
Drop cast on SiO_2	15		92.4	35.2			36.98	14.98		13
Thin films on quartz			0.73	4.1±0.3	14±3	35	227±145	252±17		14
Microwire		2.45	0.35	-155.48		3.13	114.86	64.38		15
Nanosheets		2.294±0.001	0.571±0.016		25.0±3.0	13±1	54±1	18±1	47±10	16
Nanosheets		2.285	0.597		28.011	67.2±4.1		34.4±0.8	800±0.1	17
Nanosheet								18±1		18
Single crystal						9.02	11.61	20.01	10	19
Single crystal							41.7	22.2	32	20
Single crystal Free exciton						10	38	16	46	21
Localized exciton						17	74	20	16	
Single crystal						5	42	20	0	22
Nanosheets						20.61±0.43	101.02±12.29	27.53±1.98	0	23
Nanocubes								4.6		24
Polycrystalline layers		2.78±0.23	0.235	-465±227	105±15	21.85±0.97	110.5±15.7	28.95±2.64	6.29×10^{-31}	25
Nanowire			0.054	231.1	46.7	36	204	52.4		26

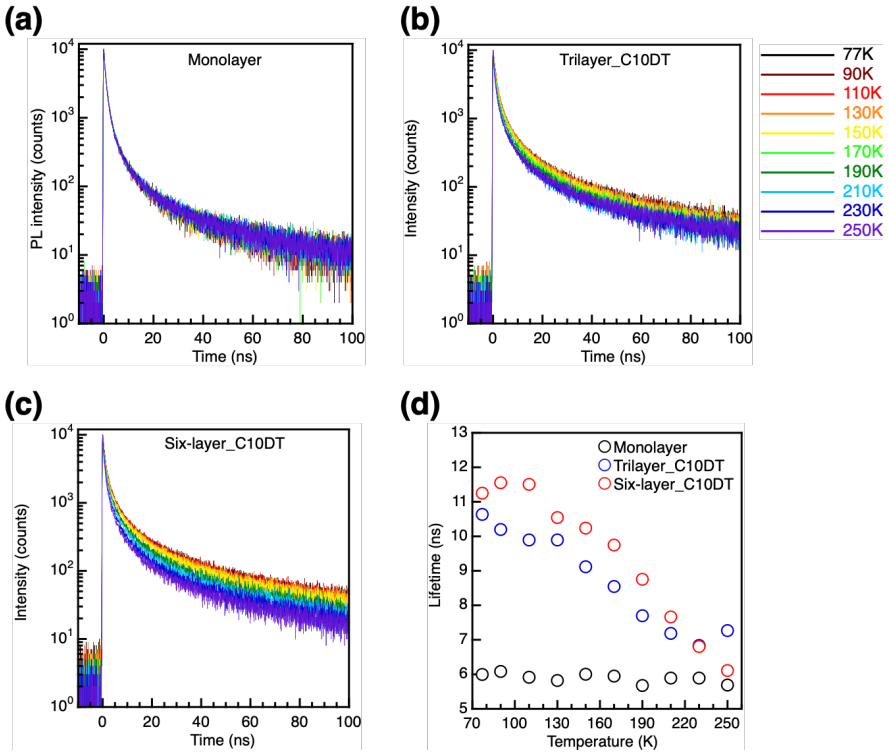

Fig. S11. Temperature dependence of transient photoluminescence (TrPL) decays of **a)** monolayer, **b)** trilayer, and **c)** six-layer prepared with C10DT. The detection energy: **a)** 2.385 eV, **b)** 2.362 eV, **c)** 2.353 eV. **d)** Temperature dependence of PL lifetime τ.

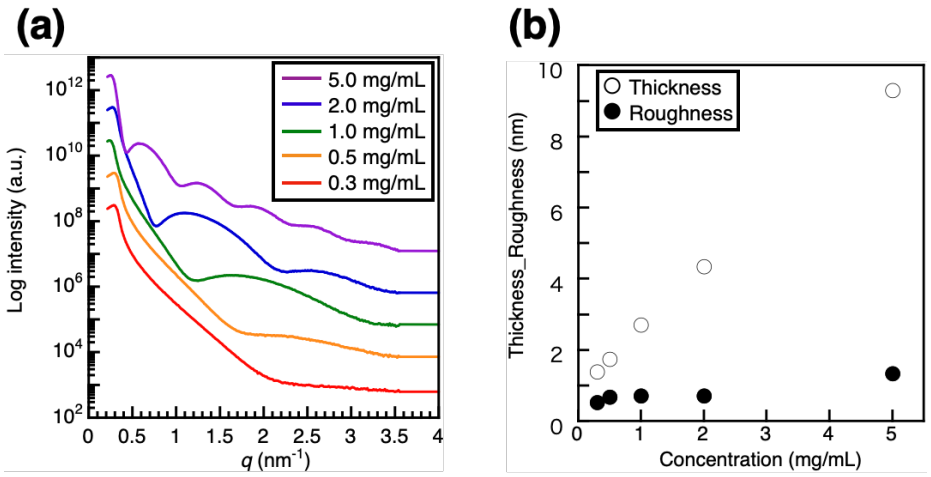

Fig. S12. **a)** X-ray reflectivity (XRR) profile of polyethylenimine (PEI) underlayer prepared with different concentrations. **b)** Concentration dependence on thickness and roughness of the underlayer.

References

1. J. Pan, L. N. Quan, Y. Zhao, W. Peng, B. Murali, S. P. Sarmah, M. Yuan, L. Sinatra, N. M. Alyami, J. Liu, E. Yassitepe, Z. Yang, O. Voznyy, R. Comin, M. N. Hedhili, O. F. Mohammed, Z. H. Lu, D. H. Kim, E. H. Sargent and O. M. Bakr, *Adv. Mater.*, 2016, **28**, 8718-8725.
2. B. A. Koscher, Z. Nett and A. P. Alivisatos, *ACS Nano*, 2019, **13**, 11825-11833.
3. D. Kim, S. Tomita, K. Ohshiro, T. Watanabe, T. Sakai, I. Y. Chang and K. Hyeon-Deuk, *Nano Lett*, 2015, **15**, 4343-4347.
4. D. Kim, S. Okahara, M. Nakayama and Y. Shim, *Phys. Rev. B*, 2008, **78**. 239901.
5. O. H. C. Cheng, T. Qiao, M. Sheldon and D. H. Son, *Nanoscale*, 2020, **12**, 13113-13118.
6. X. T. Tang, D. Rossi, J. Cheon and D. H. Son, *Chem. Mater.*, 2022, **34**, 7181-7189.
7. J. Ramade, L. M. Andriambariarijaona, V. Steinmetz, N. Goubet, L. Legrand, T. Barisien, F. Bernardot, C. Testelin, E. Lhuillier, A. Bramati and M. Chamarro, *Appl. Phys. Lett.*, 2018, **112**, 072104.
8. J. Yi, X. Y. Ge, E. X. Liu, T. Cai, C. J. Zhao, S. C. Wen, H. Sanabria, O. Chen, A. M. Rao and J. B. Gao, *Nanoscale Adv.*, 2020, **2**, 4390-4394.
9. K. Wei, Z. J. Xu, R. Z. Chen, X. Zheng, X. G. Cheng and T. Jiang, *Opt. Lett.*, 2016, **41**, 3821-3824.
10. M. Gramlich, C. Lampe, J. Drewniok and A. S. Urban, *J Phys. Chem. Lett.*, 2021, **12**, 11371-11377.
11. B. T. Diroll, H. Zhou and R. D. Schaller, *Adv. Funct. Mater.*, 2018, **28**, 1800945.
12. X. Y. Zhang, X. Gao, G. T. Pang, T. C. He, G. C. Xing and R. Chen, *J. Phys. Chem. C*, 2019, **123**, 28893-28897.
13. X. Y. Zhang, G. T. Pang, G. C. Xing and R. Chen, *Mater. Today Phys.*, 2020, **15**, 100259.
14. H. Long, X. Peng, K. B. Lin, L. Q. Xie, J. X. Lu, B. P. Zhang, L. Y. Ying and Z. H. Wei, *Appl. Phys. Express*, 2019, **12**, 052003.
15. C. R. Zhang, J. J. Duan, F. F. Qin, C. X. Xu, W. Wang and J. Dai, *J. Mater. Chem. C*, 2019, **7**, 10454-10459.
16. X. Z. Lao, W. Zhou, Y. T. Bao, X. R. Wang, Z. Yang, M. Q. Wang and S. J. Xu, *Nanoscale*, 2020, **12**, 7315-7320.
17. X. Z. Lao, Z. Yang, Z. C. Su, Z. L. Wang, H. G. Ye, M. Q. Wang, X. Yao and S. J. Xu, *Nanoscale*, 2018, **10**, 9949-9956.
18. X. Z. Lao, Z. Yang, Z. C. Su, Y. T. Bao, J. Zhang, X. Wang, X. D. Cui, M. Q. Wang, X. Yao and S. J. Xu, *J. Phys. Chem. C*, 2019, **123**, 5128-5135.
19. F. Tang, Z. C. Su, H. G. Ye, Y. Zhu, J. Y. Dai and S. J. Xu, *Nanoscale*, 2019, **11**, 20942-20948.
20. X. Z. Zhou and Z. Y. Zhang, *Aip Adv.*, 2020, **10**, 125015.
21. K. Shibata, J. Y. Yan, Y. Hazama, S. Q. Chen and H. Akiyama, *J. Phys. Chem. C*, 2020, **124**, 18257-18263.
22. Y. S. Guo, O. Yaffe, T. D. Hull, J. S. Owen, D. R. Reichman and L. E. Brus, *Nat. Commun.*, 2019, **10**, 1175.
23. Z. Yang, M. Q. Wang, H. W. Qiu, X. Yao, X. Z. Lao, S. J. Xu, Z. H. Lin, L. Y. Sun and J. Y.

Shao, *Adv. Funct. Mater.*, 2018, **28**, 1705908.

24. X. M. Li, Y. Wu, S. L. Zhang, B. Cai, Y. Gu, J. Z. Song and H. B. Zeng, *Adv. Funct. Mater.*, 2016, **26**, 2435-2445.
25. H. Cho, C. Wolf, J. S. Kim, H. J. Yun, J. S. Bae, H. Kim, J. M. Heo, S. Ahn and T. W. Lee, *Adv. Mater.*, 2017, **29**. 1700579.
26. Z. Liu, Q. Shang, C. Li, L. Zhao, Y. Gao, Q. Li, J.Chen, S. Zhang, X. Liu, Y. Fu and Q. Zhang, *Appl. Phys. Lett.*, 2019, **114**, 101902.